Site-specific glycosylation of Ebola virus glycoprotein by human polypeptide GalNAc-transferase 1 induces cell adhesion defects

Received for publication, August 14, 2018, and in revised form, October 31, 2018 Published, Papers in Press, November 2, 2018, DOI 10.1074/jbc.RA118.005375

Emily J. Simon and Adam D. Linstedt[1]

From the Department of Biological Sciences, Carnegie Mellon University, Pittsburgh, Pennsylvania 15213

Edited by Gerald W. Hart

The surface glycoprotein (GP) of Ebola virus causes many of the virus's pathogenic effects, including a dramatic loss of endothelial cell adhesion associated with widespread hemorrhaging during infection. Although the GP-mediated deadhesion depends on its extracellular mucin-like domain, it is unknown whether any, or all, of this domain's densely clustered *O*-glycosylation sites are required. It is also unknown whether any of the 20 distinct polypeptide GalNAc-transferases (ppGalNAc-Ts) that initiate mucin-type *O*-glycosylation in human cells are functionally required. Here, using HEK293 cell lines lacking specific glycosylation enzymes, we demonstrate that GP requires extended *O*-glycans to exert its deadhesion effect. We also identified ppGalNAc-T1 as largely required for the GP-mediated adhesion defects. Despite its profound effect on GP function, the absence of ppGalNAc-T1 only modestly reduced the *O*-glycan mass of GP, indicating that even small changes in the bulky glycodomain can cause loss of GP function. Indeed, protein-mapping studies identified a small segment of the mucin-like domain critical for function and revealed that mutation of five glycan acceptor sites within this segment are sufficient to abrogate GP function. Together, these results argue against a mechanism of Ebola GP–induced cell detachment that depends solely on ectodomain bulkiness and identify a single host-derived glycosylation enzyme, ppGalNAc-T1, as a potential target for therapeutic intervention against Ebola virus disease.

Ebola virus (EBOV)[2] poses a significant public health risk as evidenced by the severe outbreak in 2014–2015 that spread to several continents and multiple emerging outbreaks detected in the years since. With mortality rates as high as 90% following infection, an effective drug intervention is sorely needed. As of now, no vaccine against EBOV has been approved for widespread use, and no therapeutic options exist to specifically combat Ebola virus disease. A deeper understanding of the pathogenesis of this disease will open new avenues for therapeutic development.

Ebola virus disease is partially characterized by uncontrolled inflammation and endothelial damage, often resulting in hypovolemic shock, multiorgan failure, and death. The EBOV surface glycoprotein (GP), the only viral gene product on the virus membrane, is instrumental in causing many of these effects, including a dramatic loss of cell adhesion in infected tissues (1), and induction of pro-inflammatory signals (2, 3). Expression of GP alone in endothelial tissue explants results in loss of vascular integrity caused by reduced cell adhesion, recapitulating the symptoms observed in infected patients (1). Similarly, experiments in cultured cells show that expression of GP results in cell rounding and detachment, and the severity of rounding reflects the known virulence of different Ebola species (4, 5). Thus, the cell culture adhesion effects are a proxy for a key aspect of the complex symptoms seen with human infection. Significantly, all of these deadhesion effects depend upon the presence of the extracellular mucin-like domain (MLD) of GP (1, 6), which contains dense clusters of sites predicted to be modified by mucin-type *O*-glycosylation (7). The resulting large, bulky mass of the *O*-glycosylated MLD is believed responsible for deadhesion caused by steric blocking of surface adhesion molecules (8).

Mucin-type *O*-glycosylation, hereafter termed simply *O*-glycosylation, is a ubiquitous post-translational modification of proteins traversing the secretory pathway. *O*-Glycosylation begins in the Golgi apparatus with the addition of a GalNAc sugar onto a serine or threonine (occasionally tyrosine) residue by a polypeptide GalNAc transferase enzyme (ppGalNAc-T) (9). Humans express 20 distinct genes encoding the initiating enzymes (ppGalNAc-T1–T20). Although each of these isozymes adds an identical modification—a GalNAc sugar—the substrate can sometimes be uniquely targeted by a particular isozyme. Substrate selectivity is a product of the glycosite sequence, the presence of preglycosylated residues near the glycosite, and the tissue-specific expression of the isoenzymes (9). The nascent *O*-glycan is then further modified by addition of other sugar moieties to extend the glycan tree or terminally capped with a sialic acid (9). Based on experiments in mice, unique defects appear in animals deleted for individual ppGalNAc-T isozymes, but for all those tested, no single isozyme is essential for life (9).

This work was supported by National Institutes of Health Grants 1R21DE026714 and UO1 CA230677 (to A. D. L.). The authors declare that they have no conflicts of interest with the contents of this article. The content is solely the responsibility of the authors and does not necessarily represent the official views of the National Institutes of Health.

This article contains Figs. S1–S4.

[1] To whom correspondence should be addressed: Dept. of Biological Sciences, Carnegie Mellon University, Pittsburgh, PA 15213. Tel.: 412-268-1249; Fax: 412-268-7129; E-mail: linstedt@cmu.edu.

[2] The abbreviations used are: EBOV, Ebola virus; GP, glycoprotein; MLD, mucin-like domain; ppGalNAc-T, polypeptide *N*-acetyl galactosamine transferase; PNGase F, peptide:*N*-glycosidase F; GAPDH, glyceraldehyde-3-phosphate dehydrogenase.

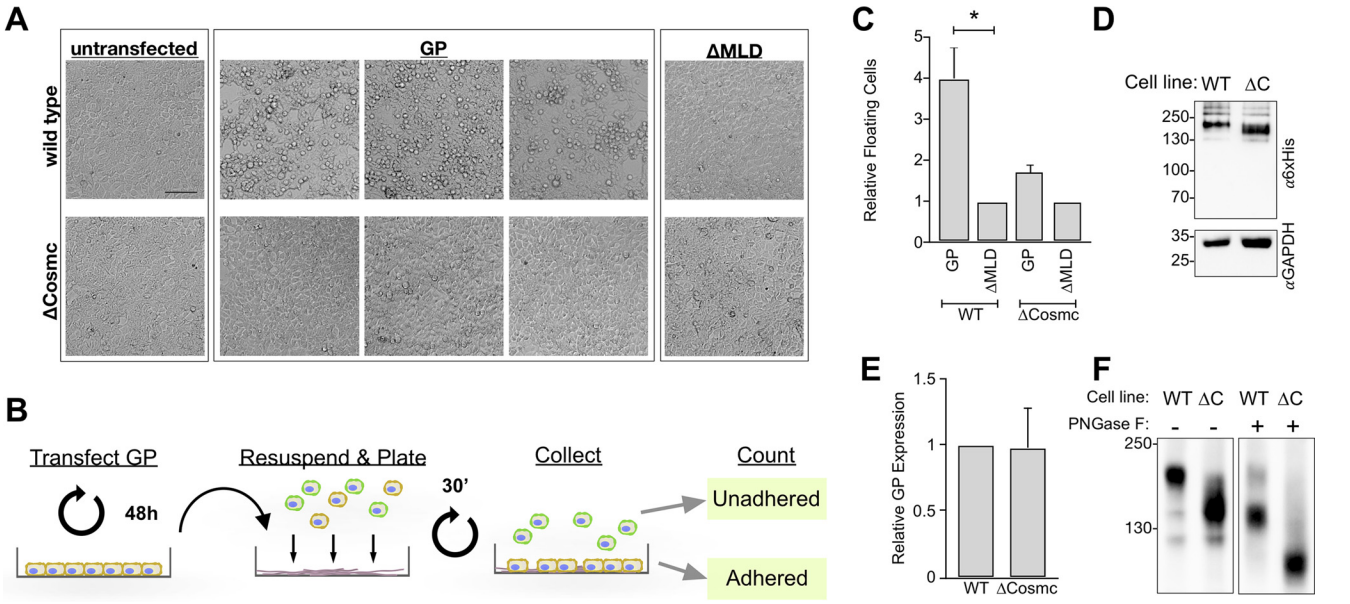

Figure 1. Extended *O*-glycans are required for GP-induced detachment. *A*, phase contrast images of WT or ΔCosmc HEK293 cells without treatment (*untransfected*) or transfected with GP or ΔMLD for 48 h. *Bar*, 10 μm. *B*, schematic of the adhesion assay. Briefly, the cells were transfected and after 48 h mechanically resuspended and plated onto a fresh collagen-coated substrate. After 30 min at 37 °C, the floating cells in the media and the adherent cells were separately collected, stained with Trypan blue, and counted. *C*, shown for each construct expressed in the indicated cell type is the normalized percentage of cells that were floating. Normalization used ΔMLD in the corresponding cell line ($n = 4 \pm$ S.E.; *, $p < 0.05$). *D*, WT and ΔCosmc (Δ*C*) lysates from the adhesion assay were immunoblotted using the indicated antibodies. *E*, intensity bands from *D* were quantified, and the GP/GAPDH ratio was plotted relative to the WT cell sample. *F*, untreated or PNGase F–treated WT and ΔCosmc (Δ*C*) cells transfected with GP were immunoblotted using anti-GP antibodies. The image is of a single membrane cropped to remove intervening lanes.

The critical role of the Ebola MLD and the selective, yet non-essential, roles of individual ppGalNAc-Ts raise the possibility of targeting the enzymes that initiate *O*-glycosylation of the MLD for novel therapeutics. However, rather than blocking *O*-glycosylation directly, previous work used relatively large deletions within the 180 residue MLD (1, 2, 5). These may cause additional defects including improper protein folding, so direct evidence of the role of *O*-glycosylation in GP function is needed. Further, elucidation of the *O*-glycosylation code is an ongoing effort, and predictive models of both *O*-glycan acceptor sites as well as isozyme selectivity toward these sites are still unreliable (7, 10). Thus, which, if any, individual ppGalNAc-T might be required for GP function must be determined experimentally.

Here we show that the *O*-glycans of GP are indeed crucial for GP-induced cell detachment and, furthermore, that ppGalNAc-T1 plays a substantial role in producing functionally competent GP. Surprisingly, however, deletion of ppGalNAc-T1 caused only slight changes in GP mass. Further, we identified a small but functionally important region within the MLD for which point mutation of its glycosites abrogated GP function. These findings identify a functionally important discrete epitope within the MLD and support targeted inhibition of *O*-glycosylation as a potential therapeutic goal for treatment of Ebola virus disease.

Results

GP requires extended O-glycans to inhibit cell adhesion

To test the hypothesis that *O*-glycans are required for GP function, we took advantage of a HEK293 cell line that has been genome edited to block expression of core 1 β3GalT-specific molecular chaperone (Cosmc) (11). Cosmc is an essential chaperone for glycoprotein-GalNAc 3-β-galactosyltransferase (C1GalT1), an enzyme required for extension of most if not all *O*-glycans in HEK293 cells. Cosmc knockout (ΔCosmc) cells lack extended mucin-type glycan trees beyond the initial GalNAc or GalNac with sialic acid (10, 11). *N*-Glycosylation and other types of *O*-glycosylation are unaffected (12). Complete inhibition of *O*-glycosylation was not feasible because it would require deletion of all 20 of the genes encoding the ppGalNAc-Ts that initiate *O*-glycosylation. Although two inhibitors of ppGalNAc-transferases were recently identified, one is selective for ppGalNAc-T3 (13), and the other, though more broadly selective, also does not affect all ppGalNAc-Ts (14). A better-known *O*-glycosylation inhibitor, benzyl-α-GalNAc, acts similarly to the ΔCosmc approach in that it prevents *O*-glycan extension by competitively inhibiting C1GalT1. In our tests, this compound proved too toxic for use (data not shown).

To begin, GP was expressed in WT HEK293 cells. As expected based on previous work (1, 5), GP expression caused widespread cell rounding and detachment (Fig. 1*A*, *top row*). This effect depended on the mucin-like domain because GP with the mucin-like domain deleted (ΔMLD) showed little effect (Fig. 1*A*, *top row*). The ΔMLD construct served as a baseline in our experiments to exclude contributions, if any, to cell rounding from parts of GP outside the MLD. Next, GP was expressed in ΔCosmc cells. Strikingly, this resulted in almost no cell rounding (Fig. 1*A*, *bottom row*). Indeed, the level of apparent cell rounding was indistinguishable from that of cells expressing ΔMLD.

To provide a quantitative measure of attachment defects, an adhesion assay was conducted. Cells were mechanically

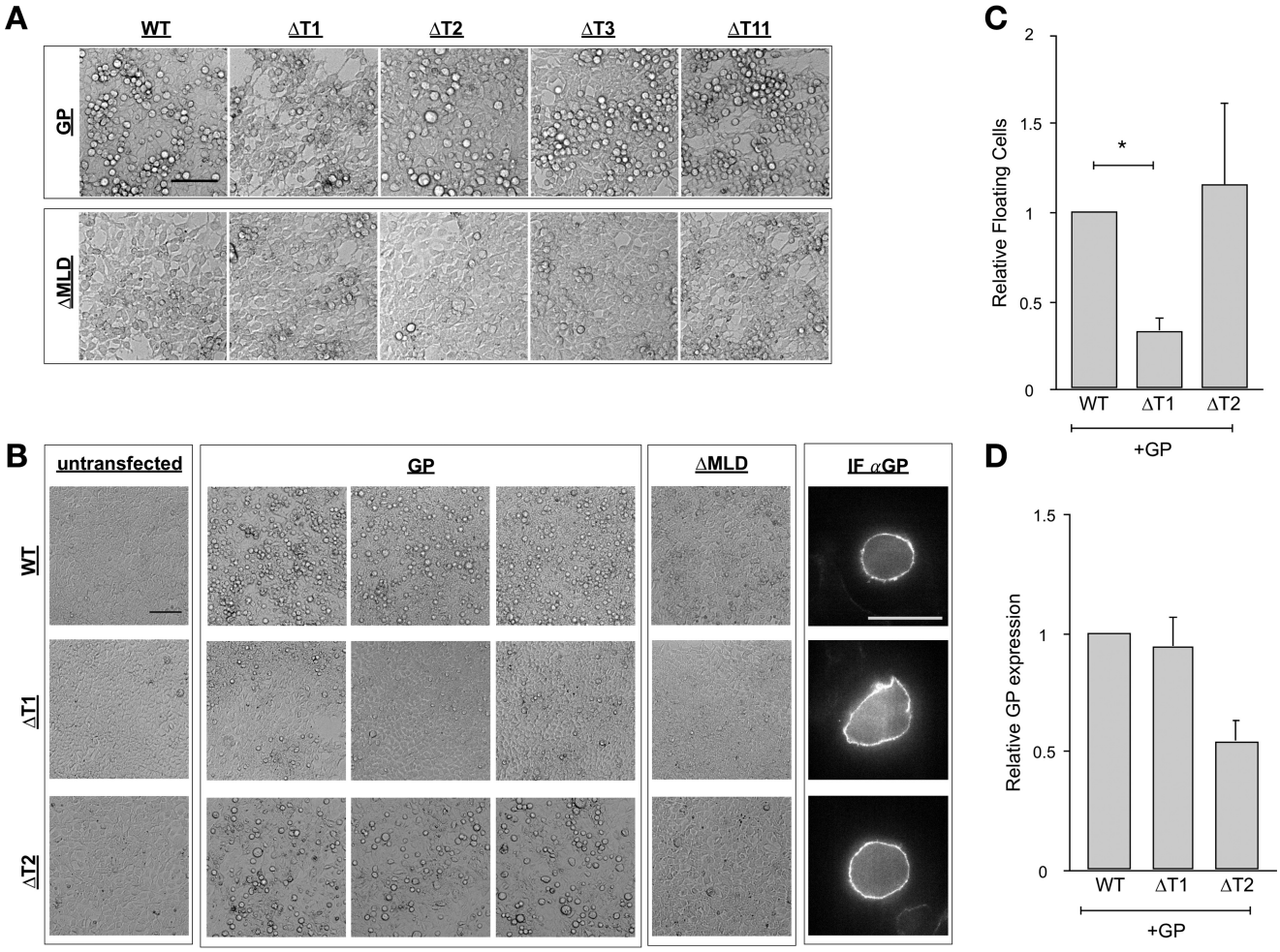

Figure 2. ppGalNAc-T1 is required for GP-induced cell rounding and loss of adhesion. *A*, phase contrast images of the indicated HEK293 cell lines expressing either GP or ΔMLD construct for 48 h. *Bar*, 10 μm. *B*, phase contrast (*left*) and immunofluorescence (*right*) images of the indicated cell lines either untransfected or transfected with GP or ΔMLD. The immunofluorescence (*IF*) is a single confocal slice of unpermeabilized cells stained using anti-GP antibodies. *Bar*, 100 μm. *C*, adhesion assay results for GP expressed in the indicated cell type showing the normalized percentage of cells that were floating. Normalization used the value for GP in WT cells ($n = 4 \pm$ S.E.; *, $p < 0.02$). *D*, immunoblot data from the adhesion assay are plotted as GP/GAPDH ratio relative to the WT cell sample ($n = 4 \pm$ S.E.). Between WT and ΔT1 expression, $p = 0.98$.

harvested 48 h post-transfection and replated on a collagen-coated surface for 30 min, after which floating and adherent cells were separately counted (Fig. 1*B*). This provided a sensitive test of the effect of GP expression on cell adherence to a substrate. For WT cells, GP significantly increased the unadhered cell fraction over that of ΔMLD, whereas for ΔCosmc cells, the effect of GP was markedly reduced (Fig. 1*C*). To ensure that differences were not due to varied expression level, cell lysates of WT and ΔCosmc cells were immunoblotted using antibodies against the His_6 epitope appended to the GP constructs. Quantification using GAPDH levels as an internal loading control revealed no significant difference (Fig. 1, *D* and *E*). Although the expected gel shift was present for GP lacking extended glycans, it was more apparent with an increased SDS-PAGE run time (Fig. 1*F*). Because *N*-glycosylation accounts for much of the mass of GP, this shift was even more pronounced after digestion with PNGase F, which removes *N*-glycans but not *O*-glycans (Fig. 1*F*). In summary, preventing *O*-glycan extension protects against GP's inhibition of cell adhesion.

ppGalNAc-T1 activity is required for GP-mediated cell detachment

Encouraged by this result, we next tested whether the activity of any one individual ppGalNAc-T might be crucial for GP *O*-glycosylation. A panel of available HEK293 cell lines was used, each lacking a single major ppGalNAc-T. The ΔT1, ΔT2, ΔT3, and ΔT11 cell lines were previously characterized (15–17) and generously supplied by the Clausen group. Strikingly, whereas GP appeared fully active in the ΔT2, ΔT3, and ΔT11 cell lines, it failed to cause significant rounding in ΔT1 cells (Fig. 2*A*). Background levels of rounding with ΔMLD expression were minimal for all tested cell lines. Fig. 2*B* is provided to show additional representative fields illustrating the protective effect of ppGalNAc-T1 deletion and also showing detection of surface GP as indicated by immunostaining in the absence of permeabilization (Fig. 2*B*). GP must be delivered to the plasma membrane to reduce adhesion (6), and we detected no defects in GP surface presence in WT, ΔT1, or ΔT2 cells. To quantify the effect of deleting ppGalNAc-T1, we used the adhesion assay

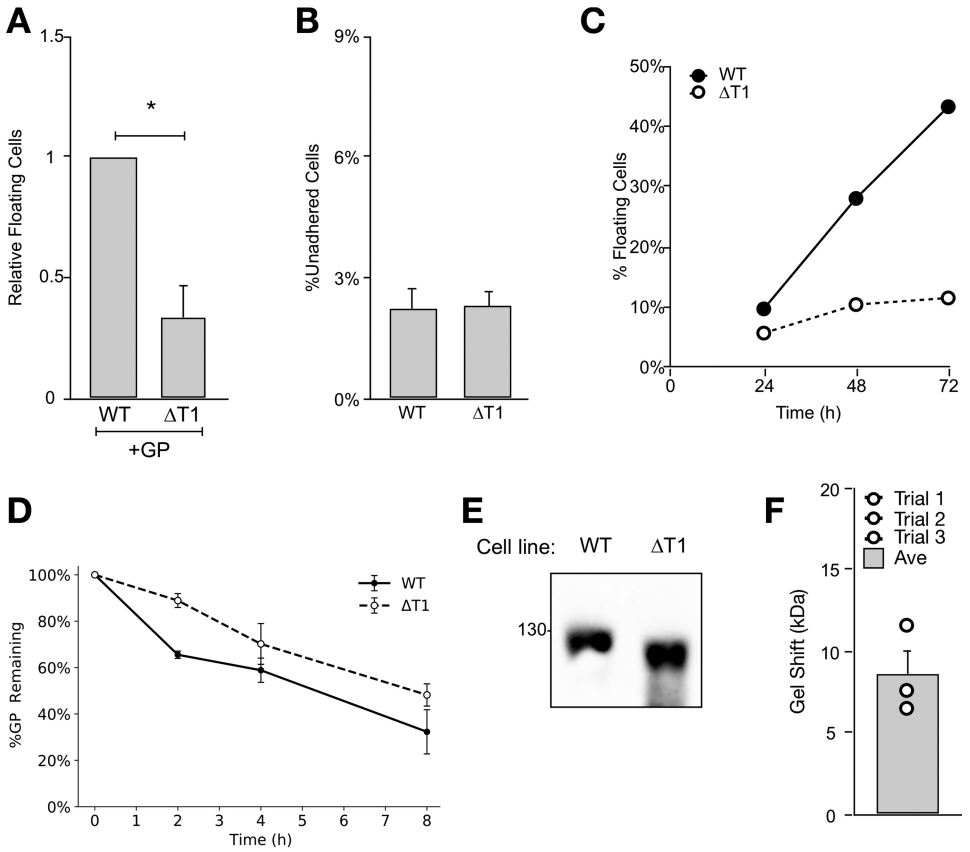

Figure 3. Altered GP glycosylation correlates with loss of deadherence activity in ΔT1 cells. *A*, results from the detachment assay for the indicated cell lines transfected with GP. The percentage of cells that were detached is plotted normalized to the WT sample ($n = 3 \pm$ S.E.; *, $p < 0.01$). *B*, the percentage of total cells that failed to readhere in the adhesion assay in the absence of transfection ($n = 3 \pm$ S.E.). *C*, the percentage of total cells that failed to readhere in the adhesion assay for the indicated cell lines at the indicated times post-transfection with GP. *D*, quantified immunoblot showing GP level in WT or ΔT1 cell lines after the indicated time of cycloheximide addition. Experiments were started 48 h after transfection immunoblotting using anti-His antibodies ($n = 3 \pm$ S.E.). *E*, untreated or PNGase F–treated WT and ΔT1 cells transfected with GP were immunoblotted using anti-GP antibodies. *F*, quantified gel shifts of PNGase F–treated samples for three independent trials, as in *E*. The average downward gel shift from WT to ΔT1 samples is 8.57 kDa, and this shift was statistically significant ($p < 0.05$). *Dots* represent a gel shift from a single trial, and the *bar* indicates the average shift ($n = 3 \pm$ S.E.).

described above. In direct comparison with GP-transfected WT and ΔT2 cells, the ΔT1 cells showed significantly reduced levels of nonadherent cells (Fig. 2*C*). This was not due to reduced expression level because quantification of immunoblots showed indistinguishable GP expression between WT and ΔT1 cells (Fig. 2*D*).

Only a subset of the O-glycans on GP are added by ppGalNAc-T1

As a complement to the adhesion assay, ΔT1 cells were also compared with WT cells in a cell detachment assay. Here, plated cells were transfected with GP, and after 48 h, floating cells were collected and quantified separately from adherent cells. This is a stringent assay because, beyond rounding or readherence, the cells must break all pre-existing contact with neighbors and the substrate. Consistent with results from the adhesion assay, the absence of ppGalNAc-T1 protected against the effects of GP in promoting detachment (Fig. 3*A*). Previous work shows that HepG2 cells lacking ppGalNAc-T1 show changes to ~10% of the glycoproteome, compared with WT cells (18). To test whether these differences might affect ΔT1 adhesion properties and artifactually account for the protection we observed, the adhesion assay was carried out in the absence of GP expression. No difference was observed (Fig. 3*B*). We also considered whether expression in ΔT1 simply delayed the effect of GP. However, a time course of GP expression using the adhesion assay showed that loss of adhesion in WT cells was approximately linear over time following transfection, whereas it remained low in ΔT1 cells (Fig. 3*C*). We also tested whether the stability of GP was altered in ΔT1 cells. Using cycloheximide to inhibit GP synthesis and reveal its degradation rate, we found no significant difference in turnover rates between the two cell lines (Fig. 3*D*). Thus, the overall level, turnover rate, and localization of GP are comparable in ΔT1 cells and cannot account for the reduced adhesion defects.

To confirm that ppGalNAc-T1 glycosylates GP, we tested for a gel shift for GP expressed in ΔT1 cells. The samples were treated with PNGase F to remove *N*-glycans and maximize detection of a shift caused by *O*-glycans. A significant downward shift of 8.6 kDa was observed for GP from ΔT1 cells, as compared with GP from WT cells (Fig. 3, *E* and *F*). Thus, some *O*-glycans on GP are in fact initiated by ppGalNac-T1, but the small magnitude of the shift indicates that these are relatively few in number (compare the shift in Fig. 3*E* with that in Fig. 1*F*). The large loss of function conferred by a small change in mass suggests that the bulk of the glycan mass on the MLD, still present in the absence of ppGalNAc-T1, is not sufficient for GP function.

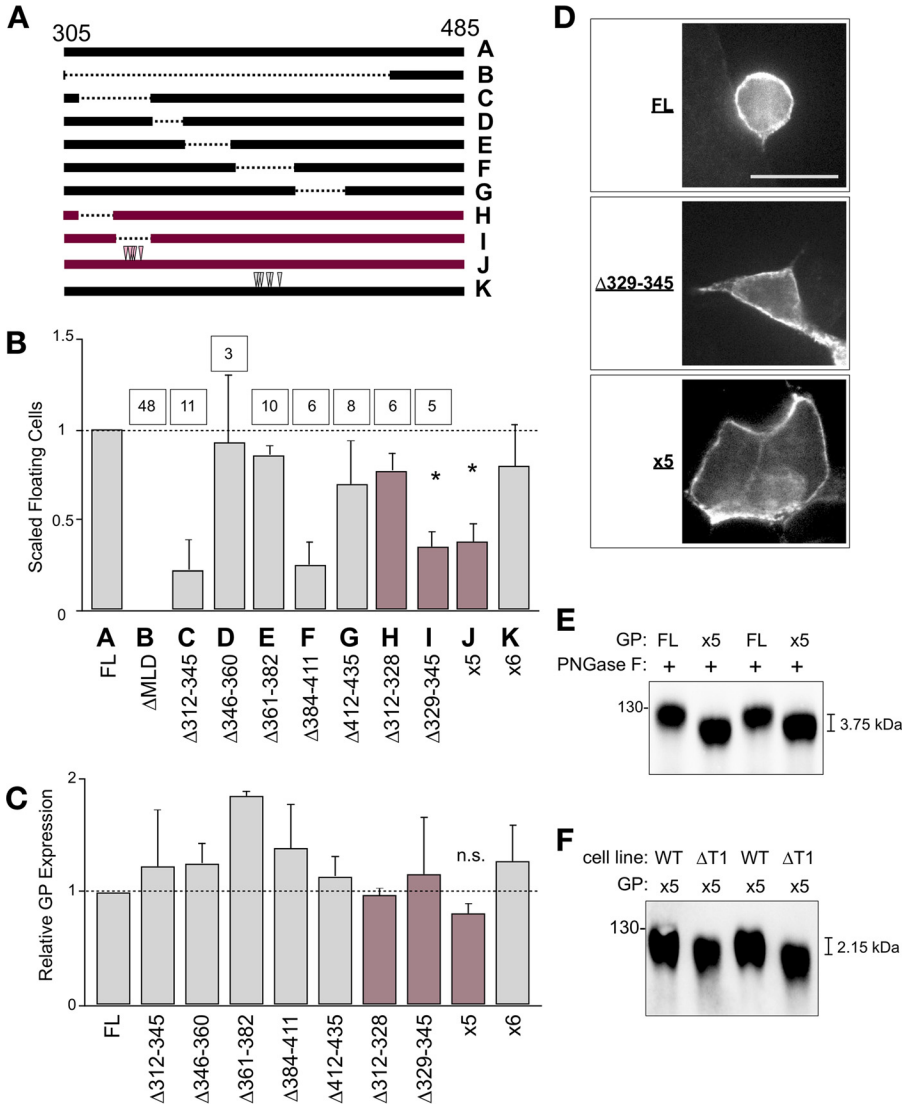

Figure 4. GP cell detachment activity requires defined segments and glycan sites within the MLD. *A*, schematic of the MLD for the constructs used with deletions (*dashes*) and point mutations (*arrowheads*) indicated. *Constructs H–J* (*magenta*) were used to refine *construct C*. The amino acid substitutions in x5 are S332G, S334A, S335G, S336G, and S344G. The substitutions in x6 are S387G, T388A, T391A, S399A, T402A, and T411A. *B*, adhesion assay data for the indicated constructs in WT HEK293 cells, where *FL* indicates full-length, WT GP. The percentage of floating cells was scaled, such that full-length GP = 1 and ΔMLD = 0 ($n = 2 \pm$ S.E.; *, $p < 0.05$ (*versus* FL)). *Boxes* indicate the number of serine or threonine (potential *O*-glycan acceptors) lost with the indicated deletion. *Letters* map to the schematics in *A*. *C*, immunoblot data from the adhesion assay are plotted as GP/GAPDH ratio relative to the FL GP sample ($n = 2 \pm$ S.E.). *D*, single confocal slice images of immunofluorescence staining of the indicated constructs in permeabilized cells using anti-His antibodies. *Bar*, 10 μm. *E*, PNGase F–treated WT cells expressing full-length GP (*FL*) or the x5 construct (*x5*) were immunoblotted using anti-GP antibodies. *F*, as in *E*, PNGase F–treated WT or ppGalNAc-T1 knockout cells expressing the x5 mutated GP construct.

Identification of glycosylation sites in the MLD required for GP deadhesion activity

To test whether discreet and functionally important glycosites could be identified within the MLD, we used a mutationally based mapping approach, building on the work of Simmons *et al.* (5). A set of nonoverlapping deletions was created in GP spanning the MLD (Fig. 4*A*). Each construct was expressed in WT cells and tested using the adhesion assay. Two regions were identified, residues 312–345 and 384–411, whose deletion potently reduced the deadhesion activity of GP (Fig. 4*B*). Significantly, flanking regions of deletion did not show the same effect.

Although deletion of the segment 384–411 impaired GP function, this was not due to its *O*-glycosylation. Point mutation of all six potential *O*-glycan sites within this segment to prevent their glycosylation yielded a construct, labeled *x6*, with full deadhesion activity indistinguishable from that of full-length GP (Fig. 4, *A–C*). Based on this result, we focused on the 312–345 segment.

The 312–345 segment was bisected to further pinpoint a required region, resulting in two additional constructs: Δ312–328 and Δ329–345. Although each deletion was of 16 residues, only 329–345 blocked GP-mediated deadhesion (Fig. 4*B*). Note that neither the number of potential *O*-glycan sites (*boxed* in the figure) nor the length of the deleted segments correlated with the degree of defect. Because 329–345 contained only five potential glycan sites, we introduced point mutations at all five sites. This final construct (labeled *x5*) therefore comprised the

full length of GP with a loss of only 5 of the potential 56 *O*-glycosylation sites in the MLD. Remarkably, this construct was significantly impaired in its ability to induce adhesion defects (Fig. 4*B*). The expression level of this construct did not significantly differ from that of WT GP (Fig. 4*C*), nor did it show a loss of plasma membrane localization (Fig. 4*D*). Further, following PNGase F treatment, a clear gel shift was observed for the x5 construct when compared with full-length GP (Fig. 4*E*). This observation confirms that *O*-glycans are normally added at one or more of these functionally required sites.

As a test of whether the mutated sites in the x5 construct encompass all of the ppGalNAc-T1 sites in GP, the x5 construct was expressed in ΔT1 cells. We reasoned that additional sites would be indicated by a further downward gel shift. Indeed, a further shift was observed, but it was only 2 kDa (Fig. 4*F*). Because this shift was smaller than the 9-kDa shift for full-length GP expressed in ΔT1 cells, the result suggests that ppGalNAc-T1 acts at several of the sites within the 329–345 segment and only a few outside of it. Consistent with this finding, there was no further functional deficit for the x5 construct when it was expressed in ΔT1 cells (data not shown). Although a small change may have been missed because of the statistical certainty of the assay, the 329–345 segment appears to contain most, if not all, of the functionally important ppGalNAc-T1 sites.

Discussion

The MLD of the Ebola GP is critical for many of the virus' pathogenic effects, including hemorrhaging, which in turn is caused partly by a loss of cell adhesion. Here we show that without extended *O*-glycans, GP cannot modulate adhesion. Further, not all sites of *O*-glycosylation on GP are required equally. Rather, GP-induced cell detachment depends on glycans added by ppGalNAc-T1 and on glycosites found in a particular region of the MLD. These findings provide direct evidence of *O*-glycan contribution to GP function and suggest that GP-mediated cell deadhesion is due to selective MLD glycosites rather than its nonspecific *O*-glycan bulk. The findings also identify ppGalNac-T1 as a potential therapeutic target.

The requirement for *O*-glycosylation of GP, shown here by preventing glycan extension, substantiates previous work that had deleted the entire MLD (1, 2, 5). As mentioned above, deletions of the protein backbone may result in undesired effects on protein structure. A complete block of *O*-glycosylation might also affect structure, particularly rigidity, because clustered *O*-glycans can provide a basis for rigid conformations and for protein stability (19). Preservation of the initial GalNAc and attached sialic acid, as is the case for ΔCosmc cells (10, 11) may retain the structural characteristics of the MLD, while additionally preserving any functional role of the protein backbone itself. Therefore, we attribute the significance of the MLD in GP-induced deadhesion to its *O*-glycans.

There are two major hypotheses regarding how *O*-glycosylation regulates GP function. The prevailing view is that glycan bulk in the MLD sterically blocks cell adhesion interactions. Alternatively, the MLD's deadhesion activity may depend on specific glycan determinants, which require a full glycan structure to be recognized by host factors that regulate adhesion. The favored hypothesis is partly based on the finding that antibodies against the cell adhesion molecule β1-integrin fail to bind their surface antigen in the presence of GP, and this masking effect is reversed with deglycosylation of the cell surface (8). Further, the trimeric umbrella-like structure of the GP ectodomain is suggestive, particularly given that its overhanging regions are comprised of the bulky densely packed MLD *O*-glycans (8, 20, 21). One would expect this mechanism of inhibition to be insensitive to the absence of just a few of the many possible glycans. Thus, our observation of functional deficit from removal of select glycans by mutation or by ppGalNAc-T1 deletion supports the idea that there may be specific glycan-based epitopes within the MLD that are needed for its deadhesion activity. In this light, it is noteworthy that deadhesion activity is retained by a chimeric construct of transmembrane-anchored MLD that is monomeric, rather than trimeric (6).

To cause cell deadhesion, GP may activate signaling pathways that modulate cell adherence. GP is known to cause signaling in pathways involved in the inflammatory response, and this activity is present in the shed form of the ectodomain (2, 3). Future work that precisely identifies the sites and structures of the functionally relevant GP glycans will be an important step in obtaining a mechanistic understanding of their role in GP-induced cell detachment. Recent advances in MS-based identification of glycosites unique to particular ppGalNAc-T isozymes will likely be critical in this endeavor (7, 10, 18, 22, 23).

Regardless of the mechanism of GP-induced deadhesion, it is significant that protection is conferred by blocking a single ppGalNAc-T isozyme. ppGalNAc-T1 is expressed across all tissue types and organs tested (9), suggesting that its inhibition could be effective across the broad range of host tissues susceptible to Ebola infection. Although inhibition of all mucin-type *O*-glycosylation would cause severe side effects (12), selective inhibition of ppGalNAc-T1 may be tolerable, especially if it is titrated by dose and time. Mice lacking ppGalNAc-T1 are viable and even fertile despite defects in blood clotting and bone development (24). Other functions that involve ppGalNAc-T1 are basement membrane deposition (25) and extracellular matrix remodeling (26). The best characterized ppGalNAc-T1–specific substrates are two heavily *O*-glycosylated proteins involved in bone deposition and remodeling, bone sialoprotein, and osteopontin (27). There are at least 55 other glycoproteins that specifically depend on ppGalNAc-T1 for their glycosylation (18), but the functional importance of their glycosylation is unknown. Although an inhibitor of ppGalNAc-T1 has not yet been characterized, recent identification of a ppGalNAc-T3 inhibitor demonstrates the strong potential for developing inhibitors against ppGalNAc-Ts that are effective and isozyme selective at nontoxic doses (13, 16).

In summary, Ebola GP requires extended *O*-glycans to cause cell detachment, and surprisingly, the loss of relatively few of these glycans, either by mutation or by deleting ppGalNAc-T1, blocks GP activity. These observations point to the possible role of specific glycan-based epitopes in the mucin-like domain that may act separately or in conjunction with nonspecific steric interference. Additionally, the requirement for ppGalNAc-T1 reveals for the first time a single glycosylation enzyme that

could be an effective therapeutic target during Ebola virus disease.

Experimental procedures

Cell lines and plasmids

All cell lines used were HEK293 (WT, ΔCosmc, ΔT1, ΔT2, and ΔT3), generously contributed by Dr. Henrik Clausen (University of Copenhagen). The cells were maintained in Dulbecco's modified Eagle's medium (Corning, Corning, NY, catalog no. 10-013-CV) containing 10% fetal bovine serum (Atlanta Biologicals, Flowery Branch, GA catalog no. S11150) at 37 °C with 5% CO_2. The plasmid encoding Zaire Ebola virus GP, strain Mayinga-76, was generously contributed by Dr. Judith White (University of Virginia). All deletion and mutation constructs were derived from this plasmid using adapted QuikChange protocols. The deletions were precise, in-frame removals of the nucleotides encoding the denoted amino acid residues (including the indicated bounding residues). These were Δ314–464 (ΔMLD), Δ312–345, Δ346–360, Δ361–382, Δ384–411, Δ412–435, Δ312–328, and Δ329–345. The point-mutated construct (x5) has the following amino acid changes: S332G, S334A, S335G, S336G, and S344G. The point-mutated construct x6 has the following amino acid changes: S387G, T388A, T391A, S399A, T402A, and T411A.

Rounding, adhesion, and detachment assays

For all assays, the cells were transfected using JETPei transfection reagent (PolyPlus Transfection, Illkirch, France, catalog no. 101) according to the manufacturer's protocol. Except for the time course, all cells were then cultured for 48 h. For the rounding assay, the cells were directly imaged using an EVOS FL cell imaging system (Invitrogen) at 10× magnification. For the adhesion assay, transfected cells were mechanically suspended (repeated gentle pipetting with a P1000 in growth medium), and $\sim 2 \times 10^6$ cells/well were transferred to a precoated 12-well plate. The plates were coated by addition of collagen coating solution (Cell Applications, San Diego, CA, catalog no. 125) for 1 h at 37 °C, two washes with PBS, and drying. After cells were transferred to coated plates, they were recultured for 30 min, and medium containing floating cells was collected. Adherent cells were trypsinized (Corning, catalog no. 25-053-Cl) without washing and collected. Aliquots of the cell solutions were diluted 1:1 with Trypan blue dye and counted with the Luna II automated cell counter (Logos Biosystems, Anyang-si, South Korea). Only dye-excluded cells were included, and the measured cell concentration was used to calculate the total number of cells per sample. Next, the percentage of unadhered cells/well was calculated (floating/(floating + adherent)). For the detachment assay, the medium containing floating cells was collected, the remaining adherent cells were trypsinized and collected, and the two samples were analyzed as described.

Immunofluorescence

Immunostaining was as previously described (28). The cells were fixed in 3% paraformaldehyde for 15 min. Blocking and antibody incubations were performed with (permeabilized) or without (unpermeabilized) 5% Triton X-100 in PBS, pH 7.4, containing 5% fetal bovine serum, 50 mM glycine. Antibodies (used at 1:1000 dilution) were anti-His (Bethyl Labs, Montgomery, TX, rabbit anti-His_6, catalog no. A190-114A) or anti-GP (IBT Bioservices, Rockville, MD, rabbit polyclonal antibody anti-ZEBOV GP, catalog no. 0301-015). The images were acquired with a 100× objective, 1.4 NA objective on a spinning confocal system (28).

Immunoblotting

To determine GP expression levels, aliquots of cells were collected from the corresponding adhesion assay, washed once with PBS, and lysed with nonreducing sample buffer. Following separation by SDS-PAGE (4–16%) and transfer onto nitrocellulose, membranes were cut between the 55 and 70-kDa markers for GP and GAPDH detection. Both were blocked for 1 h at room temperature with mild agitation in 5% nonfat dried milk in PBST (PBS + 1% Tween 20), followed by incubation with primary antibody diluted in block for 1 h. Antibodies were anti-His (see above, but used at 1:2000) and anti-GAPDH (Cell Signaling Technology, Danvers, MA, rabbit mAb GAPDH clone ^{14}C10, catalog no. 2118, 1:3000 dilution). Following five washes in PBST, membranes were incubated with horseradish peroxidase-coupled secondary antibodies, washed again, and developed using Clarity ECL (Bio-Rad, catalog no. 170-5060) according to the manufacturer's protocol. The membranes were visualized using the Bio-Rad ChemiDoc touch imaging system (catalog no. SCR-014210) and analyzed with Image Lab software. To measure GP turnover rates, cells were treated with 10 μg/ml cycloheximide in media at 37 °C for indicated times before cell lysis and blotting using anti-His antibody, as above. To assay for gel shifts, the cells were washed twice in flow wash buffer (PBS + 1% fetal bovine serum + 0.5% sodium azide) and incubated with 50,000 units/ml PNGase F (New England BioLabs, Ipswich, MA, catalog no. P0704) for 30 min at 37 °C. The cells were washed twice in flow wash buffer and lysed using reducing sample buffer and immunoblotted as above, but with anti-GP antibody (see above, 1:1000 dilution). Molecular weights were assessed using Image Lab software (Bio-Rad) using semi-log regression analysis. Images of uncropped immunoblots can found in Figs. S1–S4.

Author contributions—E. J. S. and A. D. L. conceptualization; E. J. S. data curation; E. J. S. and A. D. L. formal analysis; E. J. S. and A. D. L. funding acquisition; E. J. S. investigation; E. J. S. methodology; E. J. S. writing-original draft; E. J. S. and A. D. L. project administration; E. J. S. and A. D. L. writing-review and editing.

Acknowledgments—We thank Dr. Henrik Clausen for the generous gift of cell lines, Dr. Judith White for the generous gift of plasmids, and Dr. Marcel Bruchez for sharing microscopes. We also thank Dr. Tina Lee and Collin Bachert for insightful advice and feedback.

References

1. Yang, Z. Y., Duckers, H. J., Sullivan, N. J., Sanchez, A., Nabel, E. G., and Nabel, G. J. (2000) Identification of the Ebola virus glycoprotein as the main viral determinant of vascular cell cytotoxicity and injury. *Nat. Med.* **6,** 886–889 CrossRef Medline

2. Okumura, A., Pitha, P. M., Yoshimura, A., and Harty, R. N. (2010) Interaction between Ebola virus glycoprotein and host Toll-like receptor 4 leads to induction of proinflammatory cytokines and SOCS1. *J. Virol.* **84,** 27–33 CrossRef Medline
3. Escudero-Pérez, B., Volchkova, V. A., Dolnik, O., Lawrence, P., and Volchkov, V. E. (2014) Shed GP of Ebola virus triggers immune activation and increased vascular permeability. *PLoS Pathog.* **10,** e1004509 CrossRef Medline
4. Chan, S. Y., Ma, M. C., and Goldsmith, M. A. (2000) Differential induction of cellular detachment by envelope glycoproteins of Marburg and Ebola (Zaire) viruses. *J. Gen. Virol.* **81,** 2155–2159 CrossRef Medline
5. Simmons, G., Wool-Lewis, R. J., Baribaud, F., Netter, R. C., and Bates, P. (2002) Ebola virus glycoproteins induce global surface protein down-modulation and loss of cell adherence. *J. Virol.* **76,** 2518–2528 CrossRef Medline
6. Francica, J. R., Matukonis, M. K., and Bates, P. (2009) Requirements for cell rounding and surface protein down-regulation by Ebola virus glycoprotein. *Virology* **383,** 237–247 CrossRef Medline
7. Collar, A. L., Clarke, E. C., Anaya, E., Merrill, D., Yarborough, S., Anthony, S. M., Kuhn, J. H., Merle, C., Theisen, M., and Bradfute, S. B. (2017) Comparison of *N*- and *O*-linked glycosylation patterns of ebolavirus glycoproteins. *Virology* **502,** 39–47 CrossRef Medline
8. Francica, J. R., Varela-Rohena, A., Medvec, A., Plesa, G., Riley, J. L., and Bates, P. (2010) Steric shielding of surface epitopes and impaired immune recognition induced by the Ebola virus glycoprotein. *PLoS Pathog.* **6,** e1001098 CrossRef Medline
9. Bennett, E. P., Mandel, U., Clausen, H., Gerken, T. A., Fritz, T. A., and Tabak, L. A. (2012) Control of mucin-type *O*-glycosylation: a classification of the polypeptide GalNAc-transferase gene family. *Glycobiology* **22,** 736–756 CrossRef Medline
10. Steentoft, C., Vakhrushev, S. Y., Joshi, H. J., Kong, Y., Vester-Christensen, M. B., Schjoldager, K. T., Lavrsen, K., Dabelsteen, S., Pedersen, N. B., Marcos-Silva, L., Gupta, R., Bennett, E. P., Mandel, U., Brunak, S., Wandall, H. H., *et al.* (2013) Precision mapping of the human O-GalNAc glycoproteome through SimpleCell technology. *EMBO J.* **32,** 1478–1488 CrossRef Medline
11. Steentoft, C., Vakhrushev, S. Y., Vester-Christensen, M. B., Schjoldager, K. T., Kong, Y., Bennett, E. P., Mandel, U., Wandall, H., Levery, S. B., and Clausen, H. (2011) Mining the *O*-glycoproteome using zinc-finger nuclease-glycoengineered SimpleCell lines. *Nat. Methods* **8,** 977–982 CrossRef Medline
12. Wang, Y., Ju, T., Ding, X., Xia, B., Wang, W., Xia, L., He, M., and Cummings, R. D. (2010) Cosmc is an essential chaperone for correct protein *O*-glycosylation. *Proc. Natl. Acad. Sci. U.S.A.* **107,** 9228–9233 CrossRef Medline
13. Song, L., and Linstedt, A. D. (2017) Inhibitor of ppGalNAc-T3-mediated *O*-glycosylation blocks cancer cell invasiveness and lowers FGF23 levels. *Elife* **6,** e24051 CrossRef Medline
14. Liu, F., Xu, K., Xu, Z., de Las Rivas, M., Wang, C., Li, X., Lu, J., Zhou, Y., Delso, I., Merino, P., Hurtado-Guerrero, R., Zhang, Y., and Wu, F. (2017) The small molecule luteolin inhibits *N*-acetyl-α-galactosaminyltransferases and reduces mucin-type *O*-glycosylation of amyloid precursor protein. *J. Biol. Chem.* **292,** 21304–21319 CrossRef Medline
15. Goth, C. K., Halim, A., Khetarpal, S. A., Rader, D. J., Clausen, H., Schjoldager, K. T. (2015) A systematic study of modulation of ADAM-mediated ectodomain shedding by site-specific *O*-glycosylation. *Proc. Natl. Acad. Sci. U.S.A.* **112,** 14623–14628 CrossRef Medline
16. Song, L., Bachert, C., Schjoldager, K. T., Clausen, H., and Linstedt, A. D. (2014) Development of isoform-specific sensors of polypeptide GalNAc-transferase activity. *J. Biol. Chem.* **289,** 30556–30566 CrossRef Medline
17. Wang, S., Mao, Y., Narimatsu, Y., Ye, Z., Tian, W., Goth, C. K., Lira-Navarrete, E., Pedersen, N. B., Benito-Vicente, A., Martin, C., Uribe, K. B., Hurtado-Guerrero, R., Christoffersen, C., Seidah, N. G., Nielsen, R., *et al.* (2018) Site-specific *O*-glycosylation of members of the low-density lipoprotein receptor superfamily enhances ligand interactions. *J. Biol. Chem.* **293,** 7408–7422 CrossRef Medline
18. Schjoldager, K. T., Joshi, H. J., Kong, Y., Goth, C. K., King, S. L., Wandall, H. H., Bennett, E. P., Vakhrushev, S. Y., and Clausen, H. (2015) Deconstruction of *O*-glycosylation: GalNAc-T isoforms direct distinct subsets of the *O*-glycoproteome. *EMBO Rep.* **16,** 1713–1722 CrossRef Medline
19. Van den Steen, P., Rudd, P. M., Dwek, R. A., and Opdenakker, G. (1998) Concepts and Principles of O-Linked Glycosylation. *Crit. Rev. Biochem. Mol. Biol.* **33,** 151–208 CrossRef Medline
20. Beniac, D. R., and Booth, T. F. (2017) Structure of the Ebola virus glycoprotein spike within the virion envelope at 11 Å resolution. *Sci. Rep.* **7,** 46374 CrossRef Medline
21. Tran, E. E., Simmons, J. A., Bartesaghi, A., Shoemaker, C. J., Nelson, E., White, J. M., and Subramaniam, S. (2014) Spatial localization of the Ebola virus glycoprotein mucin-like domain determined by cryo-electron tomography. *J. Virol.* **88,** 10958–10962 CrossRef Medline
22. Bagdonaite, I., Nordén, R., Joshi, H. J., Dabelsteen, S., Nyström, K., Vakhrushev, S. Y., Olofsson, S., and Wandall, H. H. (2015) A strategy for *O*-glycoproteomics of enveloped viruses: the *O*-glycoproteome of herpes simplex virus type 1. *PLoS Pathog.* **11,** e1004784 CrossRef Medline
23. Bagdonaite, I., Nordén, R., Joshi, H. J., King, S. L., Vakhrushev, S. Y., Olofsson, S., and Wandall, H. H. (2016) Global mapping of *O*-glycosylation of varicella zoster virus, human cytomegalovirus, and Epstein–Barr virus. *J. Biol. Chem.* **291,** 12014–12028 CrossRef Medline
24. Tenno, M., Ohtsubo, K., Hagen, F. K., Ditto, D., Zarbock, A., Schaerli, P., von Andrian, U. H., Ley, K., Le, D., Tabak, L. A., and Marth, J. D. (2007) Initiation of protein *O*-glycosylation by the polypeptide GalNAcT-1 in vascular biology and humoral immunity. *Mol. Cell. Biol.* **27,** 8783–8796 CrossRef Medline
25. Tian, E., Hoffman, M. P., and Ten Hagen, K. G. (2012) *O*-Glycosylation modulates integrin and FGF signalling by influencing the secretion of basement membrane components. *Nat. Commun.* **3,** 869 CrossRef Medline
26. Tian, E., Stevens, S. R., Guan, Y., Springer, D. A., Anderson, S. A., Starost, M. F., Patel, V., Ten Hagen, K. G., and Tabak, L. A. (2015) Galnt1 is required for normal heart valve development and cardiac function. *PLoS One* **10,** e0115861 CrossRef Medline
27. Miwa, H. E., Gerken, T. A., Jamison, O., and Tabak, L. A. (2010) Isoform-specific *O*-glycosylation of osteopontin and bone sialoprotein by polypeptide *N*-acetylgalactosaminyltransferase-1. *J. Biol. Chem.* **285,** 1208–1219 CrossRef Medline
28. Mukhopadhyay, S., Bachert, C., Smith, D. R., and Linstedt, A. D. (2010) Manganese-induced trafficking and turnover of the *cis*-Golgi glycoprotein GPP130. *Mol. Biol. Cell* **21,** 1282–1292 CrossRef Medline